

Deeply Virtual Compton Scattering with Positron Beams at Jefferson Lab

Volker D. Burkert

Jefferson Lab, 26000 Jefferson Avenue, Newport News, Virginia, USA

Abstract. A brief discussion of the DVCS program at the Jefferson Lab 12 GeV energy upgrade is given. Emphasis is on what can be learned from using both polarized electron and polarized positron beams in conjunction with polarized nucleon targets.

Keywords: Positrons, DVCS, Generalized Parton Distributions

PACS: 13.60.Fz,14.60.Cd,24.70.+s,25.85.+p,25.30.Hm

INTRODUCTION

The challenge of understanding nucleon electromagnetic structure still continues after more than five decades of experimental scrutiny. From the initial measurements of elastic form factors to the accurate determination of parton distributions through deep inelastic scattering, the experiments have increased in statistical and systematic accuracy. Only during the past decade it was realized that the parton distribution functions represent special cases of a more general, much more powerful, way to characterize the structure of the nucleon, the generalized parton distributions (GPDs). For recent reviews see [1, 2].

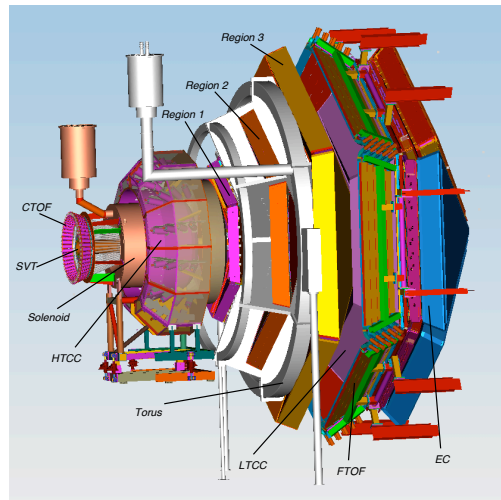


FIGURE 1. The CLAS12 detector is currently under construction to explore deeply virtual exclusive processes such as DVCS at the Jefferson Lab 12 GeV upgrade.

The GPDs are the Wigner quantum phase space distribution of quarks in the nucleon describing the simultaneous distribution of particles with respect to both position and momentum in a quantum-mechanical system. In addition to the information about the

spatial density and momentum density, these functions reveal the correlation of the spatial and momentum distributions, *i.e.* how the spatial shape of the nucleon changes when probing quarks of different momentum fraction of the nucleon.

The concept of GPDs has led to completely new methods of “spatial imaging” of the nucleon in the form of (2+1)-dimensional tomographic images, with 2 spatial dimensions and 1 dimension in momentum [3, 4]. The second moments of GPDs are related to form factors that allow us to quantify how the orbital motion of quarks in the nucleon contributes to the nucleon spin, and how the quark masses and the forces on quarks are distributed in transverse space, a question of crucial importance for our understanding of the dynamics underlying nucleon structure.

The four leading twist GPDs H , \tilde{H} , E , and \tilde{E} , depend on the 3 variable x , ξ , and t , where x is the longitudinal momentum fraction of the struck quark, ξ is the longitudinal momentum transfer to the quark ($\xi \approx x_B/(2 - x_B)$), and t is the invariant 4-momentum transfer to the proton. The mapping of the nucleon GPDs, and a detailed understanding of the spatial quark and gluon structure of the nucleon, have been widely recognized as key objectives of nuclear physics of the next decades. This requires a comprehensive program, combining results of measurements of a variety of processes in electron–nucleon scattering with structural information obtained from theoretical studies, as well as with expected results from future lattice QCD simulations. The *CLAS12* detector, shown in Fig. 1, is currently under construction to pursue such an experimental program at the Jefferson Lab 12 GeV upgrade.

ACCESSING GPDs IN DVCS

The most direct way of accessing GPDs at lower energies is through the measurement of Deeply Virtual Compton Scattering (DVCS) in a kinematical domain where the so-called handbag diagram shown in Fig. 2 makes the dominant contributions. However, in DVCS as in other deeply virtual reactions, the GPDs do not appear directly in the cross

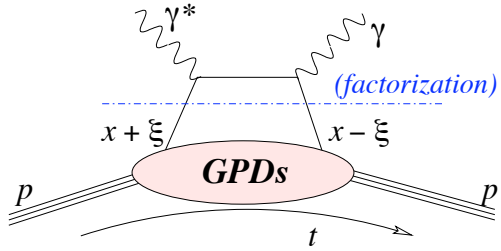


FIGURE 2. Leading order contributions to the production of high energy single photons from protons. The DVCS handbag diagram contains the information on the unknown GPDs.

section, but in convolution integrals, e.g.

$$\int_{-1}^{+1} \frac{H^q(x, \xi, t) dx}{x - \xi + i\epsilon} = \int_{-1}^{+1} \frac{H^q(x, \xi, t) dx}{x - \xi} + i\pi H^q(\xi, \xi, t), \quad (1)$$

where the first term on the r.h.s. corresponds to the real part and the second term to the imaginary part of the scattering amplitude. The superscript q indicates that GPDs depend on the quark flavor. From the above expression it is obvious that GPDs, in general, can not be accessed directly in measurements. However, in some kinematical regions the Bethe-Heitler (BH) process where high energy photons are emitted from the incoming and scattered electrons, can be important. Since the BH amplitude is purely real, the interference with the DVCS amplitude isolates the imaginary part of the DVCS amplitude. The interference of the two processes offers the unique possibility to determine GPDs directly at the singular kinematics $x = \xi$. At other kinematical regions a deconvolution of the cross section is required to determine the kinematic dependencies of the GPDs. It is therefore important to obtain all possible independent information that will aid in extracting information on GPDs. The interference terms for polarized beam I_{LU} , longitudinally polarized target I_{UL} , transversely (in scattering plane) polarized target I_{UT} , and perpendicularly (to scattering plane) polarized target I_{UP} are given by the expressions:

$$I_{LU} \sim \sqrt{\tau'} [F_1 H + \xi (F_1 + F_2) \tilde{H} + \tau F_2 E] \quad (2)$$

$$I_{UL} \sim \sqrt{\tau'} [F_1 \tilde{H} + \xi (F_1 + F_2) H + (\tau F_2 - \xi F_1) \xi \tilde{E}] \quad (3)$$

$$I_{UP} \sim \tau [F_2 H - F_1 E + \xi (F_1 + F_2) \xi \tilde{E}] \quad (4)$$

$$I_{UT} \sim \tau [F_2 \tilde{H} + \xi (F_1 + F_2) E - (F_1 + \xi F_2) \xi \tilde{E}] \quad (5)$$

where $\tau = -t/4M^2$, $\tau' = (t_0 - t)/4M^2$. By measuring all 4 combinations of interference terms one can separate all 4 leading twist GPDs at the specific kinematics $x = \xi$. Experiments at JLab using 4 to 6 GeV electron beams have been carried out with polarized beams [5, 7, 6, 8] and with longitudinal target [9], showing the feasibility of such measurements at relatively low beam energies, and their sensitivity to the GPDs. In the following sections we discuss what information may be gained by employing both electron and positron beams in deeply virtual photon production.

Differential cross section for polarized leptons

The structure of the differential cross section for polarized beam and unpolarized target is given by:

$$\sigma_{\bar{e}p \rightarrow e\gamma p} = \sigma_{BH} + e_\ell \sigma_{INT} + P_\ell e_\ell \tilde{\sigma}_{INT} + \sigma_{VCS} + P_\ell \tilde{\sigma}_{VCS} \quad (6)$$

where σ is even in azimuthal angle ϕ , and $\tilde{\sigma}$ is odd in ϕ . The interference terms $\sigma_{INT} \sim \text{Re}A_{\gamma^*N \rightarrow \gamma N}$ and $\tilde{\sigma}_{INT} \sim \text{Im}A_{\gamma^*N \rightarrow \gamma N}$ are the real and imaginary parts, respectively of the Compton amplitude. Using polarized electrons the combination $-\tilde{\sigma}_{INT} + \tilde{\sigma}_{VCS}$ can be determined by taking the difference of the beam helicities. The electron-positron charge

difference for unpolarized beams determines σ_{INT} . For fixed beam polarization and taking the electron-positron difference one can extract the combination $P_\ell \tilde{\sigma}_{INT} + \sigma_{INT}$. If only a polarized electron beam is available one can separate $\tilde{\sigma}_{INT}$ from $\tilde{\sigma}_{VCS}$ using the Rosenbluth technique. This requires measurements at two significantly different beam energies which reduces the kinematical coverage that can be achieved with this method. With polarized electrons and polarized positrons both σ_{INT} can be determined and $\tilde{\sigma}_{INT}$ can be separated from $\tilde{\sigma}_{VCS}$ in the full kinematical range available at the maximum beam energy.

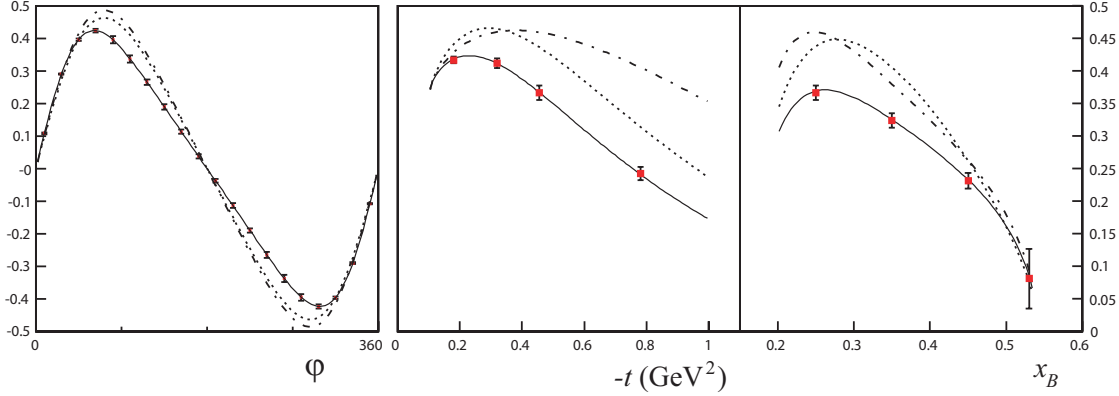


FIGURE 3. The beam spin asymmetry showing the DVCS-BH interference for 11 GeV beam energy [10]. Left panel: $x = 0.2$, $Q^2 = 3.3\text{GeV}^2$, $-t = 0.45\text{GeV}^2$. Middle and right panels: $\phi = 90^\circ$, other parameters same as in left panel. Many other bins will be measured simultaneously. The curves represent various parameterizations within the VGG model [11]. Projected uncertainties are statistical.

Differential cross section for polarized proton target

The structure of the differential cross section for polarized beam and polarized target contains the polarized beam term of the previous section and an additional term related to the target polarization [12, 13]:

$$\sigma_{\bar{e}p \rightarrow e\gamma p} = \sigma_{\bar{e}p \rightarrow e\gamma p} + T [P_\ell \Delta\sigma_{BH} + e_\ell \Delta\tilde{\sigma}_{INT} + P_\ell e_\ell \Delta\sigma_{INT} + \Delta\tilde{\sigma}_{VCS} + P_\ell \Delta\sigma_{VCS}] \quad (7)$$

where the target polarization T can be longitudinal or transverse. If only unpolarized electrons are available, the combination $-\Delta\tilde{\sigma}_{INT} + \Delta\tilde{\sigma}_{VCS}$ can be measured from the differences in the target polarizations. If unpolarized electrons and unpolarized positrons are available the combination $T\Delta\tilde{\sigma}_{INT} + \sigma_{INT}$ can be determined at fixed target polarization. With both polarized electron and polarized positron beams, the combination $T\Delta\tilde{\sigma}_{INT} + TP_\ell\Delta\sigma_{INT} + P_\ell\tilde{\sigma}_{INT} + \sigma_{INT}$ can be measured at fixed target polarization. Availability of both polarized electron and polarized positron beams thus allows the separation of all contributing terms. If only polarized electron beams are available a Rosenbluth separation with different beam energies can separate the term $\Delta\tilde{\sigma}_{INT}$ from $\Delta\tilde{\sigma}_{VCS}$, again in a more limited kinematical range. However, the term $\Delta\sigma_{INT}$ can only be determined using the combination of polarized electron and polarized positron beams.

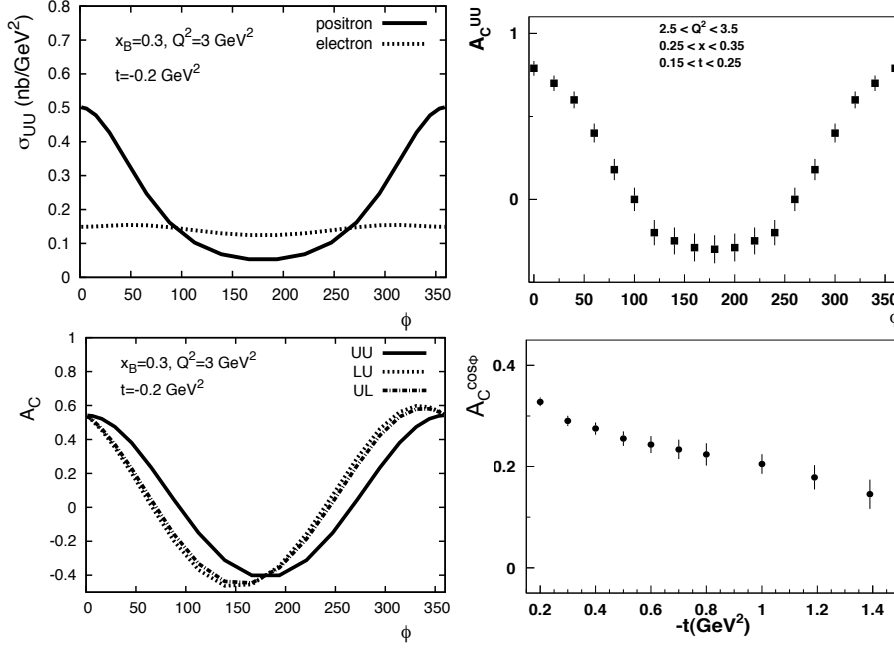


FIGURE 4. Cross sections and charge asymmetries. Top-left: Azimuthal dependence of the unpolarized cross section for positron and electron beam at 11 GeV beam energy [14]. Bottom-left: Charge asymmetries for unpolarized lepton beams (UU), for leptons at fixed polarization (LU), and for protons at fixed polarization (UL). Top-right: Projected statistical accuracy for the charge asymmetry of unpolarized lepton beams. Bottom-right: $\cos\phi$ moment of the unpolarized charge asymmetry vs momentum transfer t to the proton, for the same Q^2 and x bins as the graph at the top.

Estimates of charge asymmetries for different lepton charges

For quantitative estimates of the charge differences in the cross sections we use the acceptance and luminosity achievable with *CLAS12* as basis for measuring the process $ep \rightarrow e\gamma p$ at different beam and target conditions. A 10 cm long liquid hydrogen is assumed with an electron current of 40nA, corresponding to an operating luminosity of $10^{35}\text{cm}^{-2}\text{sec}^{-1}$. For the positron beam a 5 times lower beam current of 8nA is assumed. In either case 1000 hours of beam time is used for the rate projections. For quantitative estimates of the cross sections the dual model [14] is used. It incorporates parameterizations of the GPDs H and E . As shown in Fig. 4, effects coming from the charge asymmetry can be large. In case of unpolarized beam and unpolarized target the cross section for electron scattering has only a small dependence on azimuthal angle ϕ , while the corresponding positron cross section has a large ϕ modulation. The difference is directly related to the term σ_{INT} in (1).

CONCLUSIONS

Availability of a 11 GeV positron beam at the JLab upgrade can significantly enhance the experimental DVCS program using *CLAS12* detector in Hall B [15]. It allows access to the azimuthally even BH-DVCS interference terms that are directly related to the real part of the scattering amplitude. Moreover, by avoiding use of the Rosenbluth separation technique, the leading contributions to the cross sections may be separated in the full kinematical range available at the JLab 12 GeV upgrade. Even at modest positron beam currents of 8nA good statistical accuracy can be achieved for charge differences and charge asymmetries. For efficient use of polarized targets higher beam currents of up to 40nA are needed to compensate for the dilution factor of ~ 0.18 inherent in the use of currently available polarized proton targets based on ammonia as target material, and to allow for a more complete DVCS and GPD program at 12 GeV.

In this talk I have focussed on experiments with large acceptance detectors, which may be the only option given the low current expected for positron beams of sufficient good quality. Positron currents in excess of $1\mu\text{A}$ are likely going to be required to make such a program attractive for an experimental program with high resolution magnetic spectrometers.

ACKNOWLEDGMENTS

I would like to thank Vadim Guzey for providing me with the predictions of the minimal dual model, and Harut Avakian for the experimental projections. I also like to thank Markus Diehl for providing me with slides of his talk on the same subject in Genoa, February 2009, which I used in preparing this talk. The Jefferson Science Associates, LLT, operates Jefferson Lab under contract DE-AC05-06OR23177.

REFERENCES

1. M. Diehl, Phys. Rept. 388, 41-277, 2003, hep-ph/0307382.
2. A.V. Belitsky and A.V. Radyushkin, Phys. Rept. 418, 1-387, 2005.
3. M. Burkardt, Int. J. Mod. Phys. A18, 173-208, 2003.
4. X. Ji, Phys. Rev. Lett.91, 062001, 2003.
5. S. Stepanyan et al. (CLAS), Phys. Rev. Lett. 87, 182002, 2001, arXiv:hep-ex/0107043
6. F.X. Girod et al. (CLAS), Phys. Rev. Lett. 100, 162002, 2008, arXiv:0711.4805 [hep-ex]
7. C. Munoz Camacho et al. (Hall A), Phys. Rev. Lett. 97, 262002, 2006, arXiv:nucl-ex/0607029
8. G. Gavalian et al. (CLAS), arXiv:0812.2950 [hep-ex]
9. S. Chen et al. (CLAS), Phys. Rev. Lett. 97, 072002, 2006, arXiv:hep-ex/0605012
10. JLab experiment E12-06-119, F. Sabatie et al. (spokespersons).
11. M. Vanderhaeghen, P. Guichon, M. Guidal, Phys. Rev. D60, 094017, 1999.
12. A. Belitsky, D. Mueller, A. Kirchner, hep-ph/0112108, Nucl. Phys. B629:323-392, 2002.
13. M. Diehl, S. Sapeta, Eur.Phys.J.C41:515-533,2005, hep-ph/0503023
14. V. Guzey and T. Teckentrup, Phys. Rev. D79, 017501 (2009) (see also: <http://www.jlab.org/vguzey/>)
15. V. D. Burkert, arXiv:0810.4718 [hep-ph].